Journal of Molecular Structure 1056–1057 (2014) 285–291

Contents lists available at ScienceDirect

Journal of Molecular Structure

journal homepage: www.elsevier.com/locate/molstruc

Synthesis and characterization of nano-crystalline Zn-substituted Mg–Ni–Fe–Cr ferrites via surfactant-assisted route

W.A.A. Bayoumy *

Chemistry Department, Faculty of Science, Benha University, Benha, Egypt

HIGHLIGHTS

- Nano-crystalline Mg–Zn–Ni–Fe–CrO_4 ferrites were synthesized via surfactants-assisted route.
- The samples were characterized using XRD, FT-IR, TEM and VSM techniques.
- Surfactants type and Zn-substitution effects on different properties was studied.

ARTICLE INFO

Article history:
Received 16 June 2013
Received in revised form 19 October 2013
Accepted 20 October 2013
Available online 26 October 2013

Keywords:
Zn-substitution
Surfactant
Ferrite
XRD
TEM
VSM

ABSTRACT

Nano-crystalline ferrites of $Mg_{0.8-x}Zn_xNi_{0.2}FeCrO_4$ with stoichiometric proportion (x) lying between 0.0 and 0.8 were synthesized by sol–gel template using cationic, anionic and nonionic surfactants. The resultant powders were characterized by X-ray diffraction (XRD), Fourier transform infrared spectroscopy (FT-IR), transmission electron microscopy (TEM) and vibrating scanning magnetometry (VSM). XRD indicated the formation of polycrystalline single-phase cubic spinels with average crystallite sizes in the range of 10–15 nm. The structural data, as a function with Zn-content, has been explained on the basis of the entire cation distribution. Magnetic hysteresis loops showed very narrow hysteresis curves, which infer that the prepared powders are superparamagnetic. The smaller magnetization values obtained for all the samples can be attributed to larger surface-to-volume ratio and the spin canting on their surface. The effect of surfactant type, Zn-substitution and the presence of Cr^{3+} ions on the structural and magnetic properties of the investigated system was estimated and discussed.

1. Introduction

Nanocrystalline spinel ferrites have been the subject of many studies due to their enhanced optical, magnetic, and electrical properties, when compared with their bulk counterparts, rendering such nanoparticles of interest for a variety of applications, for example, as electrodes in energy storage devices, as catalysts, and as magnetic storage devices [1,2].

They have general formula represented by AB_2O_4 in which oxygen ions form a face-centered cubic lattice with cations occupy interstitial positions (tetrahedral A-sites and octahedral B-sites) [3]. Depending on the relative size of cations and guided by the criteria of total crystalline energy minimization of the system, the cations preferentially occupy these two sites. The compositional variation in these ferrites results in the redistribution of metal ions over the tetrahedral and octahedral sites, which can modify the properties of ferrites [4]. In addition, the low temperature synthesis, which results in the formation of nanoparticles, will have a great effect [5].

Many authors studied the effect of nonmagnetic Zn-substitution in the ferrite system such as Mg– [6], Ni– [7] and Ni–Mg [8–10] and/or magnetic Cr^{3+} ions for Fe^{3+} in $MgFe_2O_4$, $NiFe_2O_4$, $NiZnFe_2O_4$ [11–13]. These studies revealed that the substitution of magnetic Cr^{3+} (3 μ_B) for Fe^{3+} (5 μ_B) also affect magnetic properties markedly similar to that of non-magnetic substitution.

Many methods are widely investigated for the preparation of nano-sized ferrites. Some of these methods are: co-precipitation, hydrothermal, sol–gel and sol–gel auto-combustion [14,15,4]. Recently, agglomeration, which was mainly seen in wet processes, was overcome by using surfactant [16–18]. Applying surfactants, which are composed from molecules, contains of hydrophilic head and hydrophobic tail, along with sol–gel method can improve the properties of the synthesized powders. In the presence of surfactant, surface tension of solution is reduced and this facilitates nucleation and formation of the new phases [19]. The formation of reverse micelles in gel can be effective in controlling the particles growth and the distance between particles. Depending

---

* Tel.: +00201123336575.
E-mail address: wafaa_aa_bayoumy@hotmail.com

0022-2860/$ - see front matter © 2013 Elsevier B.V. All rights reserved.
http://dx.doi.org/10.1016/j.molstruc.2013.10.056

on surfactant's head electric charge, surfactants can be divided into three categories: cationic, anionic and nonionic [20,21].

To the best of my knowledge, there are no published reports on the synthesis of Zn-doped $MgNiFeCrO_4$ using surfactants. In the present study, the effect of different surfactant on the formation and magnetic properties of $Mg_{0.8-x}Zn_xNi_{0.2}FeCrO_4$ ($x = 0.0$, 0.2, 0.4, 0.6 and 0.8) nanoparticles by sol–gel template method will be investigated. The Ni content of the compositions was kept constant at 20% because the AC-resistivity was maximized near that composition [22–24].

2. Experimental procedure

2.1. Methods

Nano-sized crystals of $Mg_{0.8-x}Zn_xNi_{0.2}FeCrO_4$ ferrites (with $x = 0.0$, 0.2, 0.4, 0.6 and 0.8) were prepared by sol–gel template method using analytical grade $Mg(NO_3)_2{\cdot}6H_2O$, $Zn(NO_3)_2{\cdot}6H_2O$, $Ni(NO_3)_2{\cdot}6H_2O$, $Cr(NO_3)_2{\cdot}6H_2O$, $Fe(NO_3)_2{\cdot}6H_2O$ and citric acid as raw materials. Aqueous solutions of stoichiometric amounts of metal nitrates and citric acid are homogenously mixed with constant stirring. The molar ratio of nitrates to citric acid is 1:1. 0.005 M of cationic surfactant tetrabutyl ammonium bromide (TBAB) $\{(C_4H_9)_4NBr\}$, anionic surfactant Cyproheptadine HCl (CYP) $\{C_{21}H_{21}N.HCl\}$ or nonionic surfactant diethanol amine (dieth) $\{(CH_2CH_2OH)_2NH\}$ was dissolved in 25 ml of distilled water. The surfactants were then added to the above solution with continuous vigorous stirring at 353 K until gel formation. The obtained gels were heated at 473 K for 4 h and then calcined at 923 K for 3 h.

2.2. Instrumentation

Differential thermal analysis–thermogravimetry (DTA–TGA) measurements were carried out, using Shimadzu DT-50 thermal analyzer on precursors up to 800 °C at a heating rate of 10 °C min^{-1} in air.

XRD patterns were conducted on D8 Advance diffractometer using Cu Kα1 radiation operated at 40 kV and 35 mA.

FT-IR spectra were carried out in the range 4000–200 cm^{-1}, using a Jasco model FTIR-460 spectrometer.

TEM images were performed using JEOL 2010 transmission electron microscopy with an accelerating voltage of 100 kV.

The characteristic hysteresis loops of the system were measured at room temperature, up to a maximum external field of +8 kOe, by using vibrating sample magnetometer (VSM; Lake Shore 7404).

3. Results and discussion

3.1. Thermal analysis

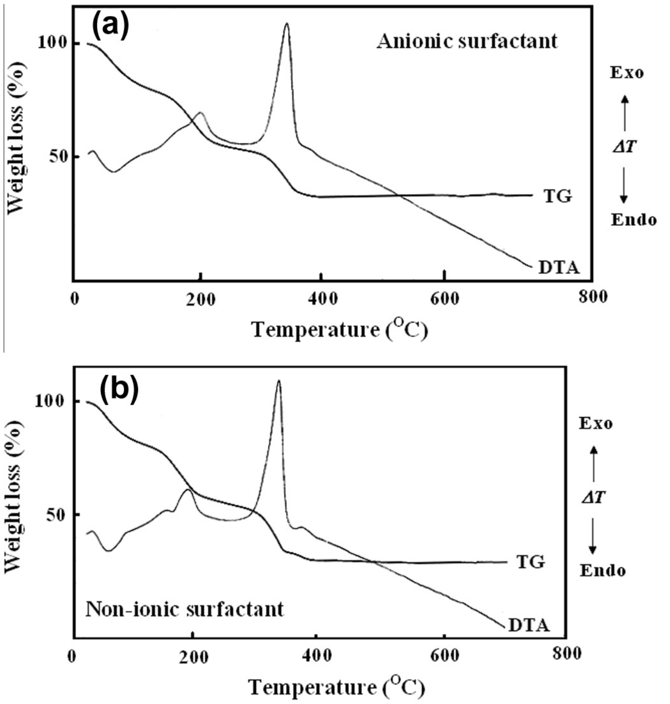

Fig. 1. DTA-TG curves in air of as-prepared precursors using (a) anionic surfactant and (b) nonionic surfactant (Heating rate = 10 °C min^{-1}).

Thermal analysis measurements were carried out to follow the precursors' decomposition and define the appropriate minimum calcination temperature, which can be considered for the complete decomposition process and the ferrite formation. Fig. 1 shows typical DTA-TG curves of precursors with $x = 0.4$, prepared using different surfactants, measured at a heating rate of 10 °C min^{-1} in air. The TG curves show successive steps, which can be attributed to the dehydration and decomposition of the nitrates–citrate–surfactants moieties. DTA curves are closely corresponding to the obtained weight losses. Generally, the first TG step in all precursors can be assigned to the precursors' dehydration since they were accompanied by endothermic DTA peaks. The exothermic DTA peaks are assigned to the decomposition of nitrates and organic contents of the precursors. No obvious weight loss can be detected above 400°C.

3.2. X-ray diffraction

X-ray diffraction patterns of the various calcined precursors are shown in Fig. 2. The reflections from the plains (220), (311), (222), (400), (422), (511) and (440), shown by all samples, indicate the formation of single-phase cubic ferrites. The broadened nature of the diffraction peaks indicates the nano-sized scale of the samples. The values of the lattice parameter (a) was calculated from the X-ray diffraction data as a function of Zn content (x) and are reported in Table 1.

From the table it is conceivable that, similar values of lattice parameters, at different zinc content, were obtained using different types of surfactant. In addition, the lattice parameters values are slightly changed with increasing Zn-content. According to Shannon [25], the ionic radius of Zn^{2+} ions (Tet.: 0.60 Å and Oct.: 0.74 Å) is slightly higher than that of Mg^{2+} ions (Tet.: 0.57 Å and Oct.: 0.72 Å). Thus, the subsequent replacement of magnesium with zinc in the investigated systems is expected to have slight effect on the values of the lattice parameters.

It is well known that, Zn^{2+} ions have a stronger preference for the tetrahedral sites, while most of the Mg^{2+} ions prefer to occupy the octahedral sites. Fe^{3+} ions can distributed between both sites though they prefer the B site while, Ni^{2+} ion exclusively occupy the octahedral site [3,26]. The Cr ions, in chromium-doped ferrites [27], are known to have strong octahedral site preference leads to the replacement of Fe^{3+} ions at this site.

Singh et al. [28] pointed that, some of the Mg^{2+} ions occupy A-site in the spinel lattice of $Ni_{0.5-x}Zn_{0.5}Mg_xFe_2O_4$ prepared by sol–gel auto-combustion technique. Mohammed et al. [29] suggested cation distribution of $(Zn_x^{2+}Mg_y^{2+}Fe_{1-x-y}^{3+})_A[Mg_{1-x-y}^{2+}Fe_{1+x+y}^{3+}]_B$ for Zn-substituted magnesium ferrite prepared by the standard double sintering ceramic method. Using Mossbauer spectroscopy and X-ray studies, the estimated cation distribution of